

03 - 27 - 06

FW

PATENT



IN THE UNITED STATES PATENT AND TRADEMARK OFFICE

Applicant : William W. Craig et al

Docket No.: IL-11099

Serial No. : 10/632,169

Art Unit: 2878

Filed : 07/30/2003

Examiner: Marcus Taningco

For : Cellular Telephone-Based Radiation Sensor and Wide-area Detection Network

Commissioner for Patents  
Alexandria, VA 22313-1450

CERTIFICATE OF MAILING UNDER 37 CFR 1.8(a)

I hereby certify that the *attached* correspondence comprising:

1. Appendix ( 8 pages)
2. Certificate of mailing (1 page)
3. Postcard

is being deposited with the United States Postal Service as express mail in an envelope addressed to:

Commissioner for Patents  
Alexandria, VA 22313-1450

on

3/23/06

Teresa Walls

(Type or print name of person mailing paper)

(Signature of person mailing paper)

BEST AVAILABLE COPY



**CERTIFICATE OF MAILING BY "EXPRESS MAIL"**

I hereby certify that this correspondence is being deposited with the United States Postal Service as express mail in an envelope addressed to: Commissioner for Patents, Alexandria, VA 22313-1450 on March 23, 2006.

3-23-06

Teresa Walls

**IN THE UNITED STATES PATENT AND TRADEMARK OFFICE**

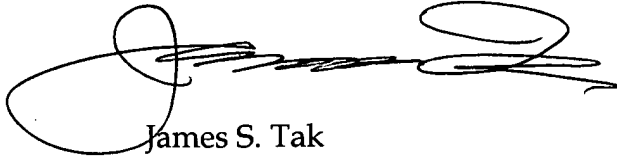
Applicants :	William W. Craig et al.	Docket No. :	IL-11099
Serial No. :	10/632,169	Art Unit :	2878
Filed :	July 30, 2003	Examiner :	Marcus H. Tanmgco
For :	Cellular Telephone-Based Radiation Sensor and Wide-area Detection Network		

Dear Sir:

Enclosed is the Appendix eight pages of a reference publication entitled, Radiation Detection and Measurement, Third Edition, by Glenn F. Koll that was inadvertently left out of the mailing of a Response to Office Action mailed September 22, 2005. Please include as part of our response to the Official Office Action.

Should you have any questions please feel to call.

Respectfully submitted,

A handwritten signature in black ink, appearing to read 'James S. Tak', with a large, stylized loop at the beginning and end.

Dated: March 23, 2006 By:

James S. Tak  
Attorney for Applicant  
Registration No. 46,367

Lawrence Livermore National Lab  
7000 East Avenue, L-703  
Livermore, CA 94550  
TEL: (925) 422-7274  
FAX: (925) 423-2231

# **Radiation Detection and Measurement**

**Third Edition**

**Glenn F. Knoll**


Professor of Nuclear Engineering and Radiological Sciences  
University of Michigan  
Ann Arbor, Michigan



John Wiley & Sons, Inc.

ACQUISITIONS EDITOR	Bill Zobrist
MARKETING MANAGER	Katherine Hepburn
SENIOR PRODUCTION EDITOR	Robin Factor
ILLUSTRATION EDITOR	Sigmund Malinowski
DESIGN DIRECTOR	Madelyn Lesure

This book was set in New Times Roman by Argosy, and printed and bound by Quebecor Printing. The cover was printed by Phoenix Color

This book is printed on acid-free paper. 

Copyright © 2000 John Wiley & Sons, Inc. All rights reserved.

No part of this publication may be reproduced, stored in a retrieval system or transmitted in any form or by any means, electronic, mechanical, photocopying, recording, scanning or otherwise, except as permitted under Sections 107 or 108 of the 1976 United States Copyright Act, without either the prior written permission of the Publisher, or authorization through payment of the appropriate per-copy fee to the Copyright Clearance Center, 222 Rosewood Drive, Danvers, MA 01923, (978) 750-8400, fax: (978) 750-4470. Requests to the Publisher for permission should be addressed to the Permissions Department, John Wiley & Sons, Inc., 111 River Street, Hoboken, NJ 07030, (201) 748-6011, fax (201) 748-6008, E-Mail: PERMREQ@WILEY.COM.

To order books or for customer service please, call 1(800)-CALL-WILEY (225-5945).

*Library of Congress Cataloging in Publication Data:*

Knoll, Glenn F.  
 Radiation detection and measurement/Glenn F. Knoll. — 3rd ed.  
 p. cm.  
 Includes index.  
 ISBN 0-471-07338-5 (cloth: alk. paper)  
 1. Nuclear Counters. 2. Radiation—Measurement. I. Title.  
 QC787.C6K56 1999  
 539.77—dc21

99-34621  
 CIP

Printed in the United States of America

10 9 8 7 6 5 4

## Appendix D

# The Shockley-Ramo Theorem for Induced Charge

Throughout this text, it has been emphasized that signals from detectors arise because of the *motion* of charge carriers after they are formed by the incident radiation. This statement generally applies to gas-filled ion chambers or proportional counters as well as to semiconductor detectors such as silicon diodes or germanium spectrometers. Those unfamiliar with the process sometimes have a naive (and incorrect) notion that the detector signal is formed only when the charge carriers deposit their electrical charges on the electrodes. That picture would imply a delay before the onset of the pulse because of the time required to transport the carriers from their point of formation to the collecting electrode. As we will see below, no such delay exists, and the output pulse begins to form immediately when the carriers start their motion to the electrodes. (Because the pulse begins as soon as the incident particle deposits its energy in the detector, the timing of detection events can be much more accurate than if a delay were to exist.) Once the last of the carriers arrives at its collecting electrode, the process of charge induction ends and the pulse is fully developed. The time evolution of the signal is of fundamental importance in understanding the timing properties of detectors as well as in predicting the effects of changes in the location of the radiation interactions on the shape of the pulse.

The derivation of the time history of the induced charge in a pulse-type ion chamber that was given in Chapter 5 was for an idealized case of a one-dimensional planar detector without boundaries or edges. For more complex geometries, a more fundamental approach is needed to carry out the analysis. There are also classes of detectors in which electrodes are subdivided into separate strips or pixels. The task of predicting the types of signals expected on a specific electrode segment also requires that a more basic approach be taken to predict induced charges. The analysis that follows will be generally applicable to all types of detectors in which charge carriers formed by radiation are caused to move in an electric field within the detector volume, including the common cases in which the active volume is either a gas or a semiconductor.

### A. Electric Potential, Electric Field, and Charge Carrier Motion

The first part of this appendix reviews the general approach to calculate the electric potential and electric field in a detector with arbitrary shape and orientation of its electrodes. The Poisson equation is the starting point for these calculations. It can be written

$$\nabla^2 \phi = \rho / \epsilon \quad (\text{D.1})$$

where  $\phi$  is the electric potential,  $\rho$  is the charge density (which may vary with position), and  $\epsilon$  is the dielectric constant for the detector medium. In the absence of trapped charges (which is usually the case for common detectors),  $\rho = 0$  and the Poisson equation reduces to the Laplace equation:

$$\nabla^2 \phi = 0 \quad (\text{D.2})$$

One must now choose the Laplacian operator  $\nabla^2$  that is appropriate for the geometry under study. In orthogonal coordinates,

$$\nabla^2 = \frac{\partial^2}{\partial x^2} + \frac{\partial^2}{\partial y^2} + \frac{\partial^2}{\partial z^2}$$

Boundary conditions needed in the solution are chosen based on the operating conditions of the detector. If an external voltage  $V$  is applied between two electrodes, then one boundary condition is that the value of the potential  $\phi$  must change by  $V$  between these electrodes. Analytical solutions are possible for some simple cases (see the development for the abrupt semiconductor junction beginning on p. 373). For complex geometries or detector shapes, solutions can be obtained only by using numerical techniques in the form of computer codes. Several commercial code packages are available that are capable of solving the Poisson or Laplace equation for complex geometries and electrode configurations. The result is a numerical solution for the electric potential  $\phi$  everywhere within the detector volume.

The electric field  $\mathcal{E}$  at any point can be obtained simply by taking the gradient of the electric potential

$$\mathcal{E} = -\text{grad } \phi \quad (\text{D.3})$$

Neglecting the effects of diffusion, charge carriers generated within the detector will follow the electric field lines (or direction of maximum gradient in the potential) from their point of formation to the collecting electrode. If an assumption is made about their velocity as a function of electric field (for example, a proportional relationship indicating a constant value of the mobility), then the position of the charge as a function of time can be uniquely determined.

## B. The Induced Charge

The general method to calculate induced charge on electrodes due to the motion of charge carriers in a detector makes use of the Shockley-Ramo Theorem<sup>1,2</sup> and the concepts of the *weighting field* and *weighting potential*. The theorem states that the instantaneous current induced on a given electrode is equal to

$$i = q\vec{v} \cdot \vec{E}_0 \quad (\text{D.4})$$

where  $q$  is the charge of the carrier,  $\vec{v}$  is its velocity, and  $\vec{E}_0$  is called the weighting field. Another way of stating the same principle is that the induced charge on the electrode is given by the product of the charge on the carrier multiplied by the difference in the weighting potential  $\phi_0$  from the beginning to the end of the carrier path:

$$Q = q\Delta\phi_0 \quad (\text{D.5})$$

To find this weighting potential  $\phi_0$  as a function of position, one must solve the Laplace equation for the geometry of the detector, but with some artificial boundary conditions:

1. The voltage on the electrode for which the induced charge is to be calculated is set equal to unity.
2. The voltages on all other electrodes are set to zero.

3. Even if a trapped charge is present within the detector volume, it is ignored in the calculation (i.e., the Laplace equation, Eq. (D.2), is used rather than the Poisson equation).

The solution under these conditions gives the weighting potential, and its gradient is the weighting field. The weighting potential is *not* the actual electric potential in the detector, but instead serves as a convenience that allows simple determination of the induced charge on the electrode of interest by taking differences in the weighting potential at the start and end of the carrier motion. The path of the carrier must still be determined from the actual electric field lines. If the position of the carrier as a function of time is determined as previously described, then the time profile of the induced charge (or the induced current) can also be traced out to determine the shape of the output pulse.

### C. Illustration: The Pixelated Detector

In Fig. D.1a, the configuration of a planar detector is sketched in which the  $x$ - $y$  surface on the left is completely covered with a conventional continuous electrode. The opposite surface has an electrode that is subdivided into a checkerboard pattern of individual pixels. Each pixel is an independent square electrode, and small gaps are present between adjacent pixels. Separate electrical contacts generally are made to each pixel electrode. We assume that no fixed charges (space charge) are present in the detector volume. For simplicity, we also assume that the dimensions of the detector in the  $x$  and  $y$  directions are large compared with the thickness  $T$ , so that edge effects can be neglected in the analysis that follows.

If a common voltage is applied on all the pixel electrodes, then the effects of the small gaps are negligible in determining the actual electric potential and electric field distributions throughout the detector volume. The results of solving the Laplace equation are then equivalent to the case in which a single continuous electrode were to replace the pixelated pattern. The potential changes linearly between the electrode-covered surfaces, and the electric field is essentially uniform throughout the volume. If the pixels are operated at a positive potential relative to the opposite surface, then negative charge carriers (electrons)

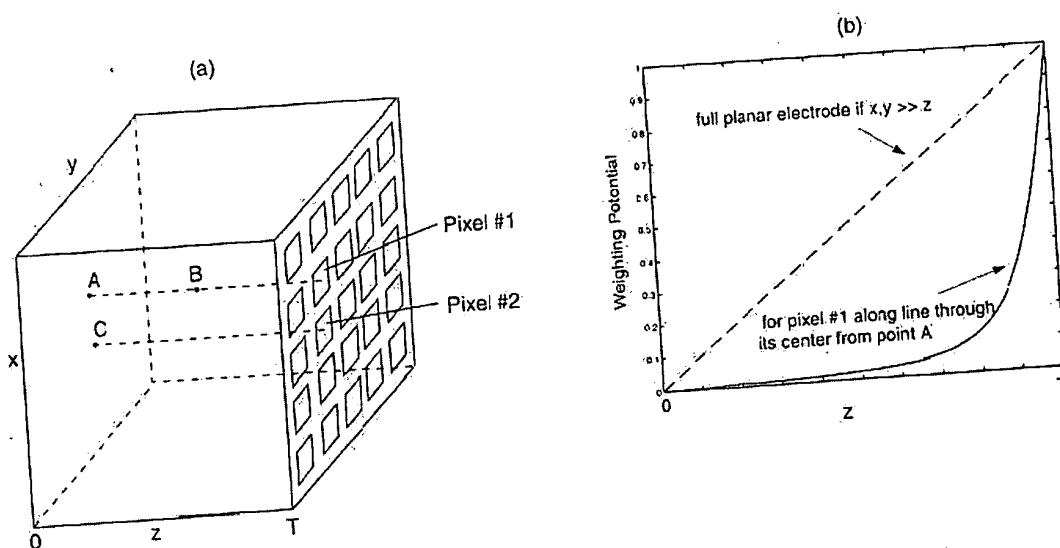


Figure D.1 (a) A planar detector configuration with a continuous cathode electrode on the  $x$ - $y$  surface at the left and a pixelated anode surface on the right. (b) Plot of the weighting potential for a continuous anode (dashed line) and for a single pixel anode (solid line), for the case in which the pixel size is 20% of the detector thickness  $T$ .



will be attracted along field lines that are parallel to each other and perpendicular to the detector surfaces. Neglecting diffusion, they will be collected by the pixel electrode that lies directly to the right of the point at which the charges are formed within the volume. The positive charges (holes or positive ions) move in the opposite direction and toward the continuous cathode at the left surface of the detector.

In order to predict the electrical signal expected from a typical single pixel electrode, we must apply the Shockley-Ramo theorem to this case to first find the configuration of the weighting potential. We again solve the same Laplace equation, but now with boundary conditions that set the potential of the pixel of interest to unity, and the potential of all other pixels and the cathode on the opposite surface to zero. The results are plotted in Fig. D.1b, and for different values of detector thickness in Fig. D.2. Notice that the shape of the weighting potential is far from linear, showing a gradient that becomes steeper at distances that are closer to the pixel electrode. Because the induced charge is proportional to the difference in weighting potential between the point of origin and collection, the electron motion will contribute much more than the motion of the positive charge for events over most of the detector volume. Only for charges created very near the pixel surface, a small fraction of the detector volume, will the positive charge motion contribute most of the charge induced on the pixel electrode. For the vast majority of events, the motion of the electron dominates the induced charge. Furthermore, it is the motion close to the pixel surface that contributes most strongly to the induced charge.<sup>†</sup> These consequences are often called the *small pixel effect*<sup>3</sup> and are most pronounced in detectors with pixel dimensions that are small compared with the detector thickness (see Fig. D.2). For detectors in which electrons are much more mobile than positive charges (such as the compound semiconductors described in Chapter 13), deriving the signal from a small pixel rather than from a large-area anode can help improve energy resolution by minimizing sensitivity of the pulse amplitude to the motion of the positive charges that may not be completely collected.

Let us now see how the Shockley-Ramo Theorem can be applied to predict the amplitude of the charge induced on one of the pixel electrodes, for the case in which the detector of Fig. D.1 is a semiconductor (to standardize the terminology). First consider the case of creating  $n_0$  electron-hole pairs from an ionizing event at a point (designated as "A" on Fig. D.1a) that is very near the cathode surface and along an axis that is perpendicular to the center of one of the pixels, call it Pixel #1. The holes will travel only a negligible distance to the cathode and will not make a significant contribution to the signals considered in this example. The induced current observed at the pixel electrode is thus due entirely to the motion of the electrons, and is initially small as the electrons move to the right through a region in which the weighting potential changes slowly (the weighting field is small). As the electrons approach the vicinity of the pixel electrode, the weighting field changes more rapidly, and the induced current rises until the electrons are collected. The electrons travel from a starting point where the weighting potential for the pixel is essentially zero to a point where it is unity (at the pixel surface.) From Eq. (D.5), the total induced charge is given by the product of the total moving charge (equal to  $-n_0e$ ) multiplied by the difference in the weighting potential between the end and the start of the electron path (unity), and is thus equal to  $-n_0e$ . This result is consistent with the prediction based on the simple conservation of energy argument given in Chapter 5 for the pulse from an ion chamber that is also applicable to planar semiconductor detectors.

Next, let us choose a more general case in which the motion of both the electrons and holes contributes to the signal. Assume that the interaction point still lies directly along the axis of Pixel #1, but now at an arbitrary depth (shown as point "B" in Fig. D.1a) where the value of the weighting potential has the value " $\beta$ " ( $0 < \beta < 1$ ). The charge induced on the

<sup>†</sup>The effect is somewhat similar to that of the Frisch grid in ion chambers described in Chapter 5, where the output signal is sensitive only to the portion of the electron motion that takes place between the grid and anode, and is free from any contributions from the positive ion motion.

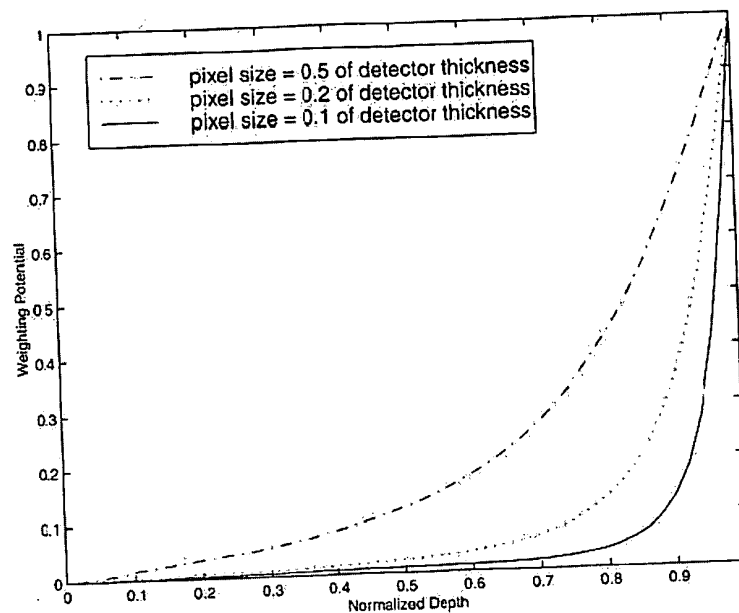
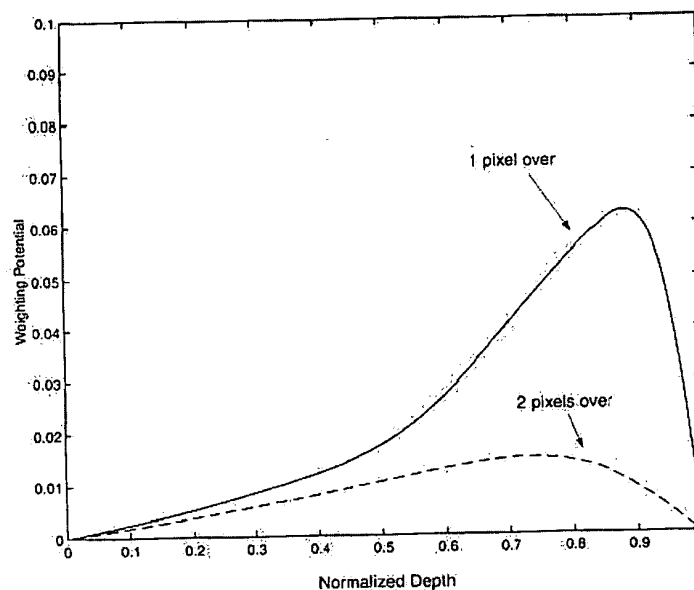


Figure D.2 Plots of the weighting potential for three different pixel electrode sizes. The small pixel effect is enhanced as the pixel size is made small with respect to the detector thickness (top and bottom curves).

pixel electrode will now have two components: one from the motion of electrons, and the other from the motion of holes. Assuming that every charge carrier is collected without loss to recombination or trapping, the total induced charge can again be predicted by applying Eq. (D.5) to both the electrons and holes. The electron motion involves a charge of  $-n_0e$  moving through a difference in weighting potential of  $(1 - \beta)$ . Thus the electron contribution to the induced charge is equal to  $-n_0e(1 - \beta)$ . The hole motion involves an equal but opposite charge of  $n_0e$  moving through a difference in the weighting potential of  $-\beta$ , so the hole contribution to the induced charge is  $-n_0e\beta$ . Combining these two contributions gives the same result as in the first case: the total induced charge is  $-n_0e$ . Thus the amplitude of the induced charge is independent of the depth at which the charges are formed, provided all carriers are fully collected.

In detectors with segmented electrodes, such as the pixelated configuration of Fig. D.1, transient signals may be induced on more than one electrode segment even when charges are created at a single point within the detector volume. Now imagine again releasing  $n_0$  electrons very near the cathode, but this time at a position (shown as point "C" on Fig. D.1a) that is along the axis of an adjacent pixel. These electrons follow the actual electric field lines that are horizontal and are collected at the Pixel #2 electrode. The weighting potential for Pixel #1 is essentially zero at the start of this path, and zero at the end, so no net charge is induced when the electrons are collected by the adjacent pixel. But notice from Fig. D.3 that along their path, the electrons pass through a region in which the weighting potential for Pixel #1 rises and passes through a maximum before dropping to zero. Thus a transient signal is induced on the Pixel #1 electrode even though the electrons never reach its surface. The induced current in this case will have a bipolar shape in which the positive and negative lobes balance to produce a net zero integrated charge. If shaped with a long integration time, the resulting pulse amplitude would also be near zero. However, if shorter shaping times are used, a pulse with finite amplitude will result that preferentially responds to the portions of the induced charge with the fastest time characteristics. These



**Figure D.3** The solid curve shows the weighting potential for Pixel #1 of Fig. D.1a along an axis that is perpendicular to the center of an adjacent pixel. The dashed line shows the same variation along the axis of a pixel that is located two pixels away. Both plots are for the case in which the pixel size is 20% of the detector thickness  $T$ . Note that the vertical scale is expanded by a factor of 10 compared with the previous two figures.

pulses that are induced on neighboring pixels that do not actually participate in collection of the charge carriers are sometimes given the apt name of "spectator pixel" signals.

In pixel detectors, the size of the induced charge on the primary pixel electrode is the same for all events that occur at positions that are within the projected area of the pixel. Thus simple positioning schemes that are based on sensing the largest pixel signal can locate the event only to within the dimensions of one pixel. The existence of induced signals on neighboring pixels opens the possibility of more precise position-sensing, since these signals will be sensitive to small changes in the exact location of the event. If all the signals in the neighborhood of the primary pixel are read out, an interpolation scheme can be implemented to more accurately position the event to within a fraction of a pixel dimension.

## REFERENCES

1. W. Shockley, *Jour. of Appl. Physics* 9, 635 (1938).
2. S. Ramo, *Proc. of the I. R. E.* 27, 584 (1939).
3. H. H. Barrett, J. D. Eskin, and H. B. Barber, *Phys. Rev. Lett.* 75, #1, 156 (1995).

**This Page is Inserted by IFW Indexing and Scanning  
Operations and is not part of the Official Record**

**BEST AVAILABLE IMAGES**

Defective images within this document are accurate representations of the original documents submitted by the applicant.

Defects in the images include but are not limited to the items checked:

- ☒ **BLACK BORDERS**
- ☐ **IMAGE CUT OFF AT TOP, BOTTOM OR SIDES**
- ☐ **FADED TEXT OR DRAWING**
- ☐ **BLURRED OR ILLEGIBLE TEXT OR DRAWING**
- ☐ **SKEWED/SLANTED IMAGES**
- ☐ **COLOR OR BLACK AND WHITE PHOTOGRAPHS**
- ☐ **GRAY SCALE DOCUMENTS**
- ☐ **LINES OR MARKS ON ORIGINAL DOCUMENT**
- ☐ **REFERENCE(S) OR EXHIBIT(S) SUBMITTED ARE POOR QUALITY**
- ☐ **OTHER:** \_\_\_\_\_

**IMAGES ARE BEST AVAILABLE COPY.**

**As rescanning these documents will not correct the image problems checked, please do not report these problems to the IFW Image Problem Mailbox.**